

OXIDATIVE PHOSPHORYLATION AND ULTRASTRUCTURAL TRANSFORMATION IN MITOCHONDRIA IN THE INTACT ASCITES TUMOR CELL

CHARLES R. HACKENBROCK, TERRY G. REHN,
EUGENE C. WEINBACH, and JOHN J. LEMASTERS

From the Department of Anatomy, The Johns Hopkins University School of Medicine, Baltimore, Maryland 21205, and The Laboratory of Parasitic Diseases, National Institute of Allergy and Infectious Diseases, National Institutes of Health, Bethesda, Maryland 20014. Dr. Hackenbrock's present address is the Department of Cell Biology, The University of Texas Southwestern Medical School at Dallas, Dallas, Texas 75235

ABSTRACT

We have examined the ultrastructure of mitochondria as it relates to energy metabolism in the intact cell. Oxidative phosphorylation was induced in ultrastructurally intact Ehrlich ascites tumor cells by rapidly generating intracellular adenosine diphosphate from endogenous adenosine triphosphate by the addition of 2-deoxyglucose. The occurrence of oxidative phosphorylation was ascertained indirectly by continuous and synchronous monitoring of respiratory rate, fluorescence of pyridine nucleotide, and 90° light-scattering. Oxidative phosphorylation was confirmed by direct enzymatic analysis of intracellular adenine nucleotides and by determination of intracellular inorganic orthophosphate. Microsamples of cells rapidly fixed for electron microscopy revealed that, in addition to oxidative phosphorylation, an orthodox → condensed ultrastructural transformation occurred in the mitochondria of all cells in less than 6 sec after the generation of adenosine diphosphate by 2-deoxyglucose. A 90° light-scattering increase, which also occurs at this time, showed a $t_{1/2}$ of only 25 sec which agreed temporally with a slower orthodox → *maximally* condensed mitochondrial transformation. Neither oxidative phosphorylation nor ultrastructural transformation could be initiated in mitochondria in intact cells by the intracellular generation of adenosine diphosphate in the presence of uncouplers of oxidative phosphorylation. Partial and complete inhibition of oxidative phosphorylation by oligomycin resulted in a positive relationship to partial and complete inhibition of 2-deoxyglucose-induced ultrastructural transformation in the mitochondria in these cells. The data presented reveal that an orthodox → condensed ultrastructural transformation is linked to induced oxidative phosphorylation in mitochondria in the intact ascites tumor cell.

INTRODUCTION

We have previously reported that the oxidative synthesis of ATP by mitochondria isolated from mouse liver (1), and from rat liver (2), parallels a rapid ultrastructural transformation in the electron-transport membrane and matrix of the mitochondria. This ultrastructural transformation, which has been designated the orthodox → condensed transformation, has been shown, by

conventional use of metabolic inhibitors and uncouplers, to be energy dependent and is thought to be a manifestation of conformational events originating in the electron-transport membrane of the mitochondrion (1, 2). Similar ultrastructural transformations appear to be driven by ion-induced osmotic perturbations (3).

Ultrastructural transformations linked to energy metabolism have now been identified in mitochondria isolated from beef heart (4) as well as from rat kidney (5). More recently, ultrastructural transformations have been observed in mitochondria *in situ* under various experimental conditions (6-8). In none of the *in situ* studies, however, was oxidative phosphorylation monitored; therefore, the relationship of mitochondrial conformation to oxidative phosphorylation in the intact cell has not been determined.

It is with these observations in mind that we have extended our studies to include an analysis of the ultrastructure of mitochondria as it relates to energy metabolism in intact cells. It should be noted that to induce, and especially to monitor, oxidative phosphorylation in intact cells is considerably more complex than to induce and monitor oxidative phosphorylation in isolated mitochondria, especially when a relationship to mitochondrial ultrastructure is sought. Whereas oxidative phosphorylation can be readily induced in isolated mitochondria by the direct addition of ADP,¹ ultrastructurally and physiologically intact cells are not permeable to ADP. Intracellular ADP, however, can be generated from endogenous ATP in ascites tumor cells via the hexokinase-linked phosphorylation of added monosaccharides such as glucose, mannose, or 2-deoxyglucose (9-12). Intracellular ADP generated in this manner is rapidly rephosphorylated to ATP by the mitochondria. Thus, the initial response of ascites tumor cells to added glucose and other hexoses is identical to the response of isolated mitochondria to added ADP, i.e., an increase in respiratory rate (10), a decrease in the reduction level of electron-

transport carriers (10), and an increase in light scattering (13), changes generally accepted as indirect evidence for oxidative phosphorylation.

In addition to monitoring these three parameters continuously and synchronously in ascites tumor cells while rapidly fixing microsamples of cells for electron microscopy, we have verified the occurrence, inhibition, or uncoupling of oxidative phosphorylation by direct enzymatic analysis of intracellular ATP, ADP, AMP, and P_i. Thus, this communication reports results obtained by monitoring oxidative phosphorylation concomitantly with the ultrastructure of mitochondria in the intact cell.

MATERIALS AND METHODS

Ehrlich ascites tumor cells were originally obtained from Doctors Mark Woods and Dean Burk, National Cancer Institute, Bethesda, Md. The cells were maintained in 25-g male Swiss mice after intraperitoneal injection. Cells in their log phase of growth were harvested from the peritoneal cavity of decapitated mice 6 days after inoculation, and then heparinized and centrifuged at 40 g for 5 min at 0°C. Only peritoneal samples essentially free of erythrocytes were used. After centrifugation, the loosely packed cells were gently diluted 1:1 by volume in the following osmotically adjusted medium which was also used as the reaction medium: 123 mM NaCl, 4.9 mM KCl, 1.2 mM MgSO₄, 16 mM Tris buffer at pH 7.4. Sucrose or additional NaCl was added to equal the osmolar concentration of the ascites fluid which was determined to be 308 mosmolar.

Protein was determined by a Biuret-cyanide procedure (14). All experiments were carried out at a protein concentration of 5 mg/ml of reaction medium. Hemocytometer counts showed that 1 mg of protein was equal to 2.4×10^6 cells.

Fluorescence emission of pyridine nucleotide (15), light scattering (13), and oxygen consumption (16) were monitored simultaneously and continuously with strip chart recorders from a Brice-Phoenix dual photomultiplier light-scattering photometer at 25°C and constant stirring speed. The tip of a Clark oxygen electrode (17) was located in the photometer cuvette just above the light path. Pyridine nucleotide was excited at 366 nm and the resulting fluorescence emission, a measure of oxidation-reduction level, was selected at 440-460 nm at 270° (15, 18). Light scattering, carried out at 546, 520, or 366 nm, was monitored at 90° (13, 19).

In order to follow rapid changes in intracellular adenine nucleotides and inorganic phosphate, consecutive samples of cells were removed from the reaction cuvette with automatic pipets and ejected into tubes containing equal volumes of 5% perchloric

¹ Abbreviations used: AMP, adenosine monophosphate; ADP, adenosine diphosphate; ATP, adenosine triphosphate; P_i, inorganic phosphate; 2DOG, 2-deoxyglucose; 2DOG-6-P, 2-deoxyglucose-6-phosphate; G-6-P, glucose-6-phosphate; DNP, dinitrophenol; FCCP, carbonyl cyanide *p*-trifluoromethoxyphenylhydrazone; NADH, reduced nicotinamide adenine dinucleotide; Ad. Nuc., total adenine nucleotide (AMP + ADP + ATP).

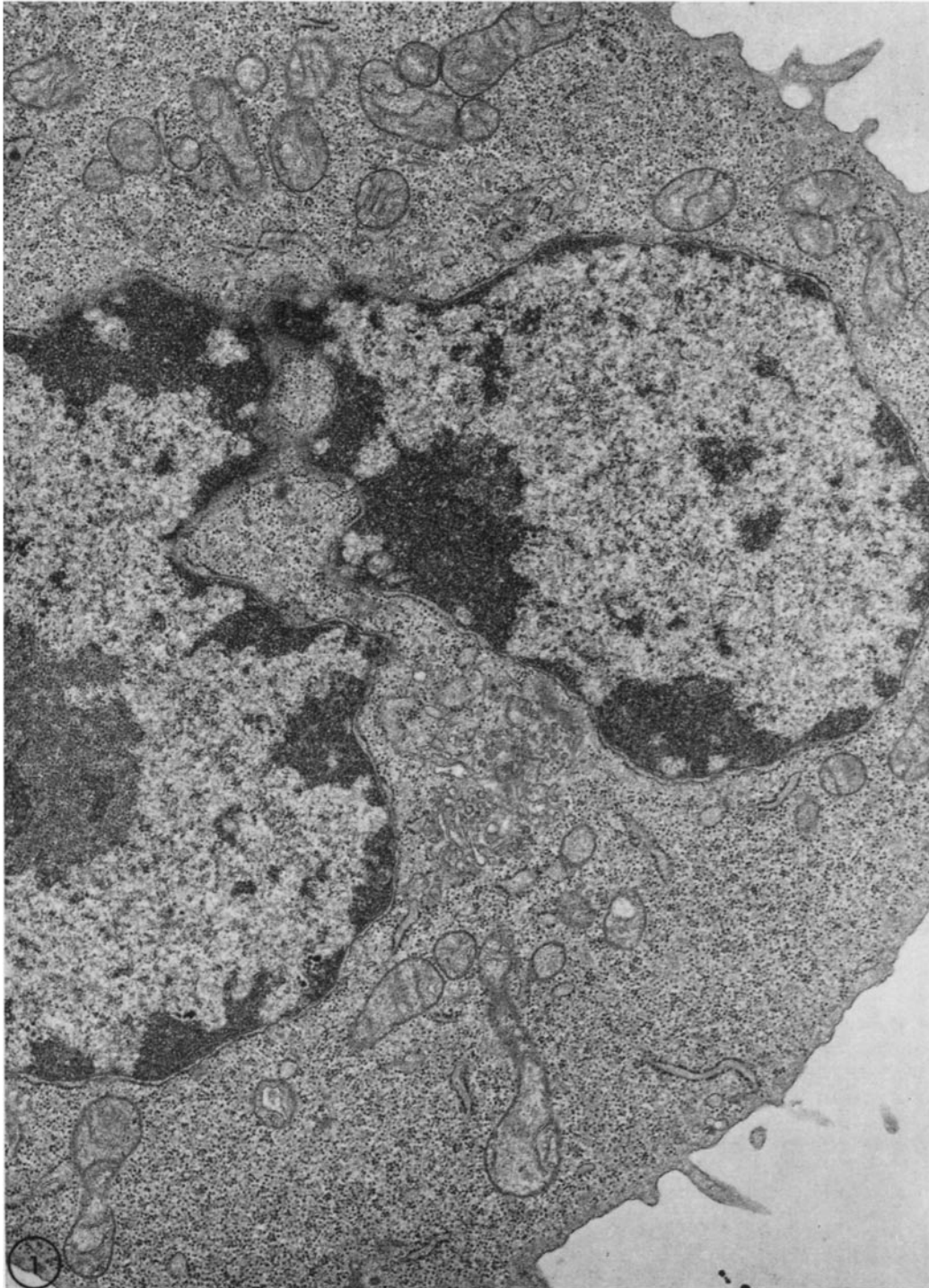


FIGURE 1 Freshly harvested, ultrastructurally intact ascites tumor cell. Mitochondria are generally rod-shaped and consistently found in the orthodox conformation. $\times 19,000$.

acid held at -4°C in ice-salt mixtures. After extraction for 30 min with intermittent manual stirring, the samples were centrifuged so as to remove the precipitated protein. The acid extracts were neutralized with a solution of 0.5 M triethanolamine and 3 M K_2CO_3 . The insoluble potassium perchlorate was removed by centrifugation and the extracts were analyzed at once. All the above steps were

carried out at -4°C . Adenine nucleotides were determined enzymatically essentially as described by Adam (20). ATP was determined on 0.5-ml samples of the neutralized extracts with phosphoglycerate kinase and glyceraldehyde-3-phosphate dehydrogenase, while ADP and AMP were determined on 0.5-ml samples with pyruvate kinase, lactate dehydrogenase, and myokinase. Changes in the absorbance of the added NADH in these determinations were measured at 340 nm with a Cary Model 15 recording spectrophotometer (Cary Instruments, Monrovia, Calif.). Enzymes were purchased from Boehringer Mannheim Corporation, New York. Standard solutions of adenine nucleotides were added after each determination in order to insure that no contamination or interfering substances were present in the test enzyme system or in the neutralized extracts, and to insure that the procedures were specifically valid for the particular nucleotide under test.

Total acid-extractable, inorganic orthophosphate was estimated on 0.5 ml samples of the extracts by the *p*-semidine procedure of Dryer et al. (21).

Consecutive microsamples of cells, averaging 0.25 mg of protein and 6.0×10^5 cells each, were rapidly removed from the reaction cuvette with Hamilton syringes and ejected into 10 times the volume of 2% glutaraldehyde in 0.1 M Na-phosphate buffer (pH 7.4). The rate of fixation was found to be 3–5 sec and was determined in parallel experiments by monitoring the cessation of respiration of intact cells after reaction with fixative. Microsamples were then left in suspension in fixative for 1 hr. This was followed by an osmotically adjusted phosphate-sucrose wash and a postfixation in 2% osmium tetroxide in 0.1 M Na-phosphate buffer (pH 7.4) for 1 hr.

Thin sections of Epon-embedded micropellets were stained for 20 min at 60°C in 1.0% sodium borate solution saturated with uranyl acetate followed by lead hydroxide 1/40 dilution for 5 min (2). Electron micrographs were taken on Kodak $3\frac{1}{4} \times 4$ in. contrast plates at an initial magnification of 7800 with an RCA 3G electron microscope operated at 50 kv and equipped with an anticontamination cold trap and double condenser.

RESULTS

Ultrastructural Transformation and Energy State

The ultrastructure of freshly harvested intact ascites tumor cells is characteristic of the high rate of cytogenesis in cancer cells in that the cytoplasm is relatively electron-opaque owing to a very high content of free ribosomes and polyribosomes (Fig.

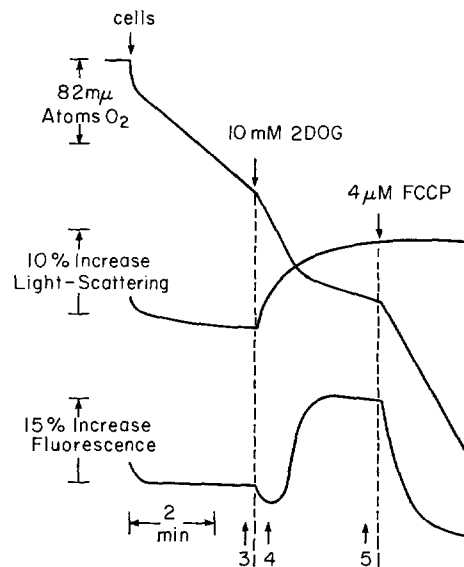


FIGURE 2 a

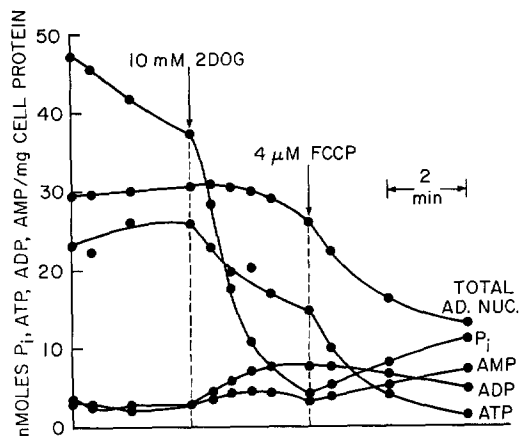


FIGURE 2 b

FIGURE 2 Metabolic response of ascites tumor cells to addition of 2DOG followed by FCCP. Fig. 2 a, Changes in oxygen consumption, fluorescence of pyridine nucleotide and 90° light scattering. Numbered arrows refer to microsamples of cells fixed for electron microscopy and shown in Figs. 3–5. Fig. 2 b, Kinetics of intracellular adenine nucleotides and P_i .

1). The sparse rough endoplasmic reticulum is arranged as monodispersed flattened cisternae. Mitochondria show the usual orthodox conformation (1) observed in most ultrastructurally intact cells.

During endogenous respiration, ascites tumor cells show steady-state levels of their 90° light-scattering property and fluorescence of pyridine nucleotides (Fig. 2 *a*). After 3 min of endogenous respiration, the orthodox conformation of the mitochondria persists (Fig. 3) and the over-all cell structure remains identical to that observed in the freshly harvested cells. Fig. 2 *a* shows that addition of 2DOG initiates a 2-fold increase in oxygen consumption, a decrease in fluorescence, which reports a decrease in the reduction level of mitochondrial pyridine nucleotide, and an increase in the light-scattering signal. Microsamples of cells fixed in suspension within 6 sec after 2DOG-induced respiratory stimulation show a rapid orthodox \rightarrow condensed ultrastructural transformation to have occurred in the mitochondria of all cells (Fig. 4). The condensed conformation is similar to that observed in phosphorylating isolated mitochondria (2). The matrix shows an increased electron opacity and a decrease in volume while the inner membrane becomes irregularly oriented. Fig. 5 illustrates *maximally* condensed mitochondria after 2DOG addition. The matrix shows a further increase in electron opacity and a further decrease in volume. Consequently, the volume of the intracristal space increases, often occupying as much as 40% of the total mitochondrial volume. Although the orthodox \rightarrow condensed transformation occurs in all cells in less than 6 sec, the rate of *maximal* condensation differs from cell to cell (Fig. 6), and parallels the rate at which the 90° light-scattering signal increases (Fig. 2 *a*). It is noteworthy that the mitochondria undergo the orthodox \rightarrow condensed ultrastructural transformation while they retain their usual rod-shaped appearance which is characteristic of structurally intact cells.

Analysis of the kinetics of intracellular adenine nucleotides and P_i (Fig. 2 *b*) shows that the 2DOG-induced increase in cellular respiration, decrease in fluorescence, increase in light scattering, and rapid condensation of mitochondria occur concomitantly with a rapid burst of ATP synthesis. The rate and extent of oxidative phosphorylation are observed in Fig. 2 *b* as a rapidly falling level of intracellular P_i while intracellular ATP is

converted to ADP during the phosphorylation of the added 2DOG.

The rapid stimulation of the oxidative synthesis of ATP by the addition of 2DOG lasts for approximately 40 sec and parallels the time-course of the decrease in fluorescence of mitochondrial pyridine nucleotide (Fig. 2 *a*). This is followed by an inhibitory phase of respiration (a Crabtree-like effect) which occurs in temporal agreement with a pronounced increase in fluorescence. The large fluorescence increase indicates a major rise in the reduction level of mitochondrial pyridine nucleotide which is to be expected to occur with inhibition of electron transport in the presence of non-glycolyzable hexose. As the 2DOG-induced inhibition of respiration sets in (Fig. 2 *a*), the intracellular level of P_i approaches zero, and the rate of phosphorylation decreases (Fig. 2 *b*) while the mitochondria maintain a maximally condensed conformation (Fig. 5). This finding agrees with earlier observations that mitochondria remain condensed in the presence of respiratory inhibitors such as Antimycin and cyanide (2). Once respiratory inhibition is established, neither the light-scattering increase nor the condensed state of the mitochondria can be reversed by subsequent release of respiratory inhibition (Fig. 2 *a*) and initiation of ATPase activity (Fig. 2 *b*) by $4 \mu\text{M}$ FCCP. Similarly, once respiratory inhibition is established, this structural state is not affected by $100 \mu\text{M}$ DNP, $50 \mu\text{M}$ Dicumarol, $5 \mu\text{M}$ Rotenone, $0.5 \mu\text{g}$ Antimycin/mg protein, or $1.6 \mu\text{g}$ oligomycin/mg protein.

Inhibition of Ultrastructural Transformation

Inhibition of the 2DOG-induced orthodox \rightarrow condensed transformation and light-scattering increase occurs when uncouplers or metabolic inhibitors are added while these changes are in progress. In addition, we have observed that if complete uncoupling is induced, the subsequent addition of 2DOG fails to effect an orthodox \rightarrow condensed mitochondrial transformation or rise in light-scattering.

Fig. 7 illustrates the uncoupling effects of $4 \mu\text{M}$ FCCP. Uncoupling is suggested by a pronounced increase in respiratory rate and decrease in mitochondrial pyridine nucleotide fluorescence (Fig. 7 *a*). Uncoupling is confirmed by a pronounced rise in the intracellular levels of P_i and ADP and a decrease in the ATP pool which is indicative of activated mitochondrial ATPase

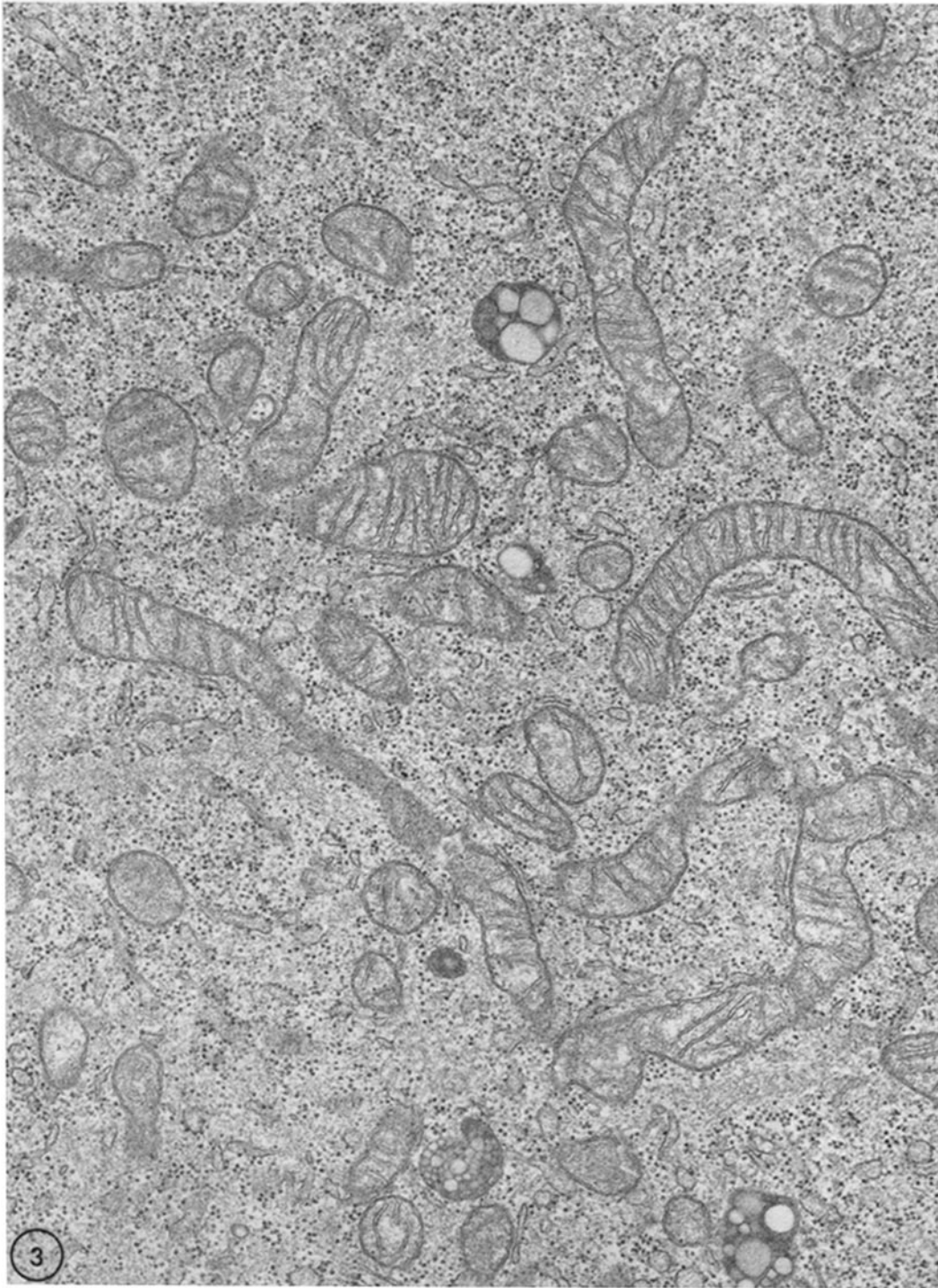


FIGURE 3 Mitochondria in intact ascites tumor cell fixed after 3 min of endogenous respiration show the orthodox conformation. (See arrow 3 in Fig. 2 a). $\times 26,800$.

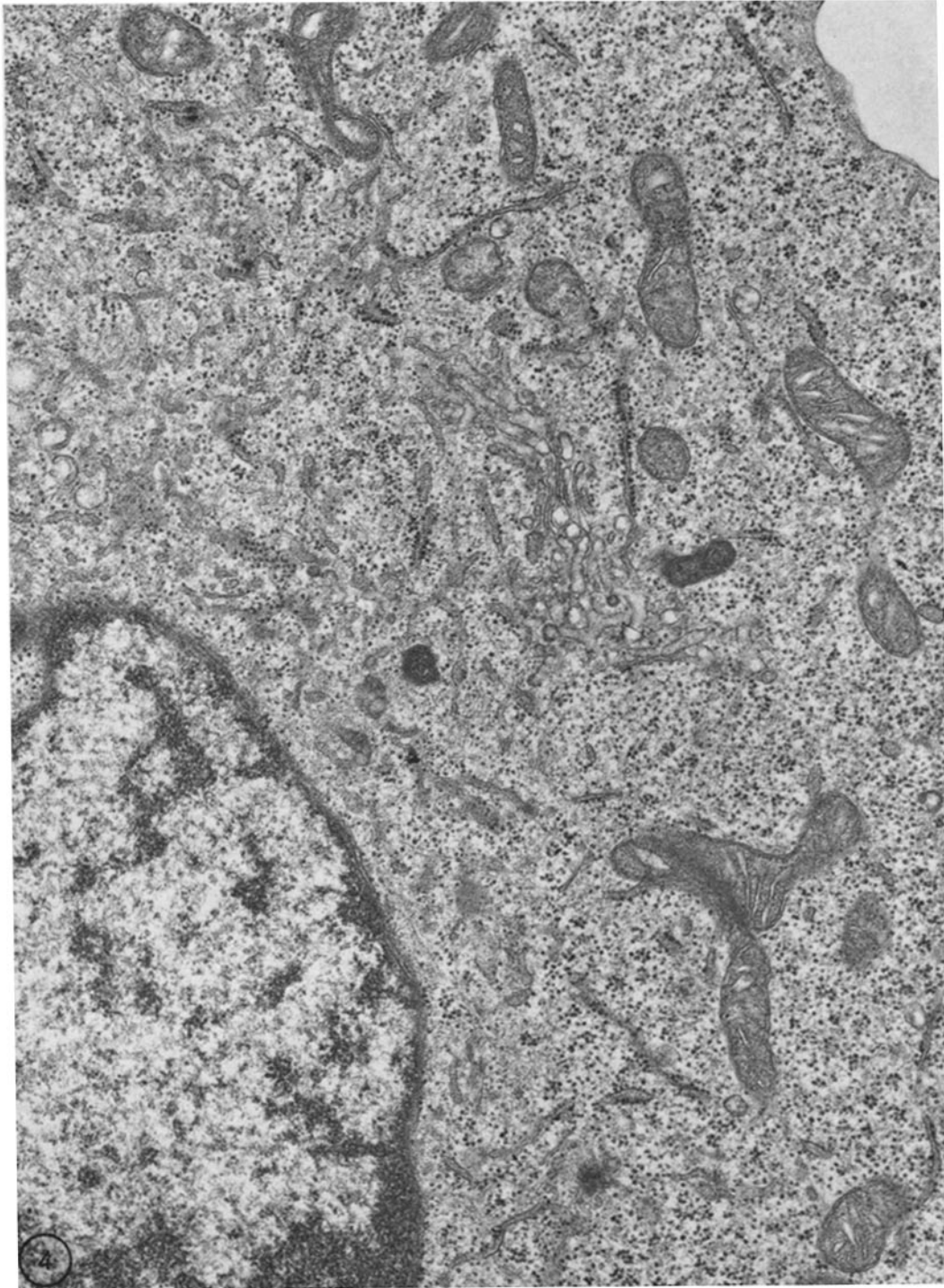


FIGURE 4 Intact ascites tumor cell fixed within 6 sec after the induced generation of intracellular ADP by addition of 2DOG. Mitochondria undergo an orthodox-to-condensed ultrastructural transformation (See arrow 4 in Fig. 2 a). $\times 26,800$.

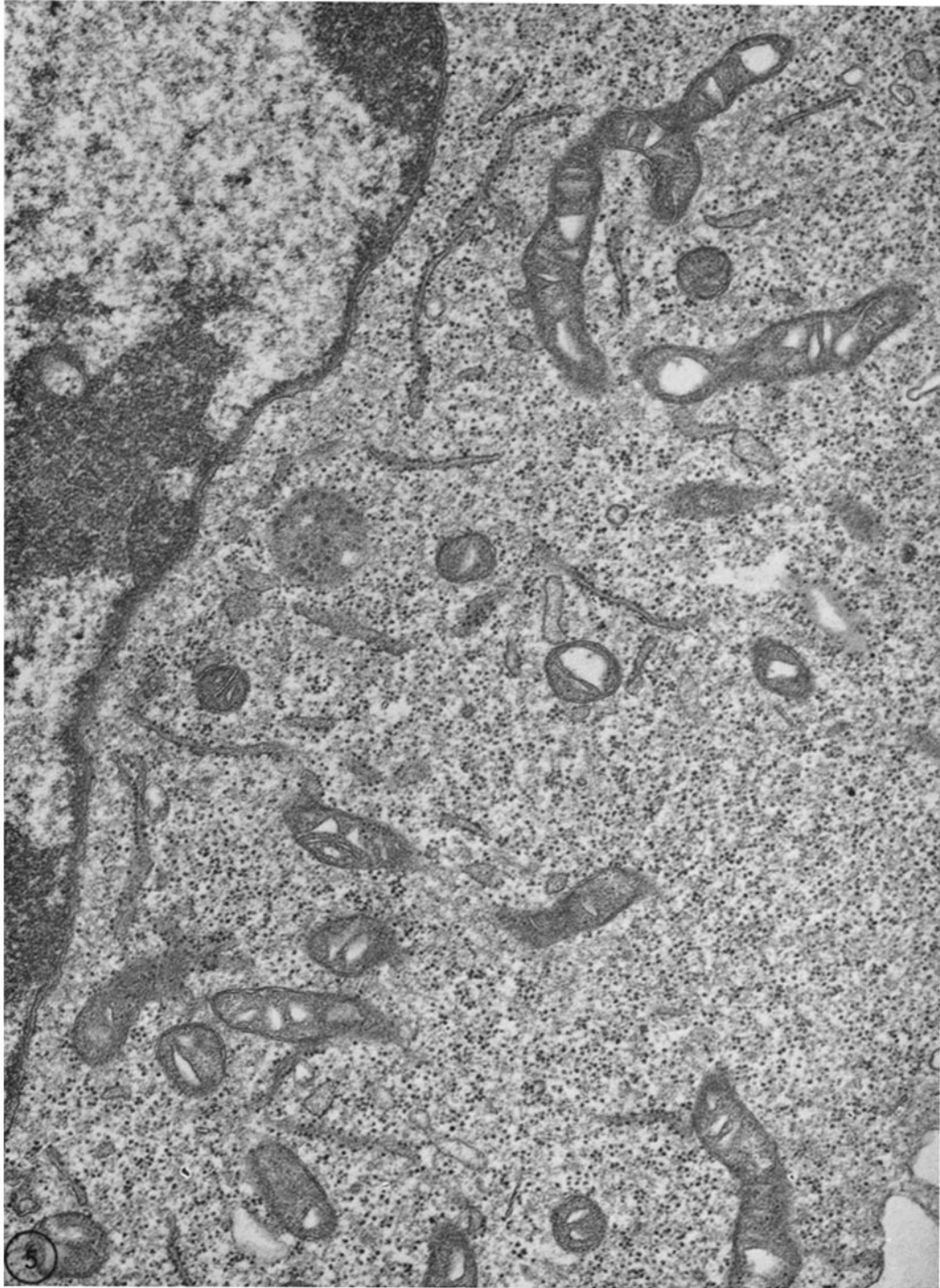


FIGURE 5 Intact ascites tumor cell fixed 3 min after the induced generation of intracellular ADP by addition of 2DOG. Mitochondria show maximal condensation (See arrow 5 in Fig. 2 a). $\times 26,800$.

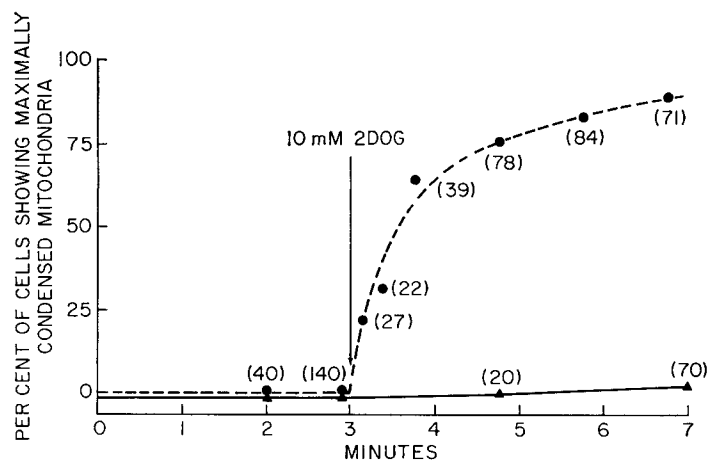


FIGURE 6 Kinetics of *maximal* condensation of mitochondria in intact ascites tumor cells after intracellular generation of ADP by addition of 2DOG. Numbers in parentheses = numbers of cells counted; ●---●, experimental; ▲—▲, control. Compare the experimental curve with the kinetics of the light-scattering rise in Fig. 2 *a*.

(Fig. 7 *b*). As expected, the FCCP-induced ATPase activity decreases with time owing to the rising ADP level. After 2 min of uncoupling, no major transformation in mitochondrial ultrastructure or change in light scattering is observed and the subsequent addition of 2DOG fails to effect an orthodox → condensed mitochondrial transformation or rise in light scattering (Fig. 7 *a*). That 2DOG does, in fact, enter the uncoupled cells and is phosphorylated is confirmed in Fig. 7 *b* by a pronounced decrease of intracellular ATP and increase of ADP. Fig. 7 *b* also shows that ATP synthesis is abolished in these cells since 2DOG fails to initiate a decrease in the intracellular P_i pool.

Ultrastructural Transformation Related to Partial and Complete Inhibition of Oxidative Phosphorylation

The relationship between the orthodox → condensed ultrastructural transformation in mitochondria and oxidative phosphorylation in the intact ascites tumor cell is exemplified in cell systems when partially inhibited ATP synthesis can be compared with totally inhibited ATP synthesis. After 3 min of endogenous respiration, the addition of 0.8 μg of oligomycin/mg of cell protein produces a 40–50% decrease in respiratory rate and, in addition, an increase in the fluorescence of mitochondrial pyridine nucleotide (Fig. 8 *a*). This

decrease in respiration is paralleled by a decrease in intracellular ATP and a rise in P_i and ADP levels (Fig. 8 *b*) indicative of the rate of consumption of endogenous ATP stores for cellular functions.

No pronounced change in light scattering (Fig. 8 *a*) or mitochondrial ultrastructure (Fig. 9) occurs with the oligomycin-linked respiratory decrease and fluorescence increase. However, a subsequent addition of 2DOG effects a partial increase in light scattering (Fig. 8 *a*) which parallels a less than maximal orthodox → condensed ultrastructural transformation in the mitochondria of the intact cells (Fig. 10). Only a few cells show *maximally* condensed mitochondria under these conditions. Although no change in respiration or pyridine nucleotide fluorescence is observed at this time (Fig. 8 *a*), we have consistently found that a small degree of ATP synthesis takes place which is revealed by a reversal and plateauing of the rising level of intracellular P_i (Fig. 8 *b*). That 2DOG initiates a pulse of ATP synthesis under these inhibitory conditions is supported by a control curve (Fig. 11) which shows an uninhibited rise of intracellular P_i when 2DOG is not added after oligomycin. The lack of respiratory stimulation during this ATP synthesis is suggestive of a loss of acceptor control under these conditions.

Thus, the relationship between ATP synthesis and the orthodox → condensed transformation is maintained even under conditions of partial in-

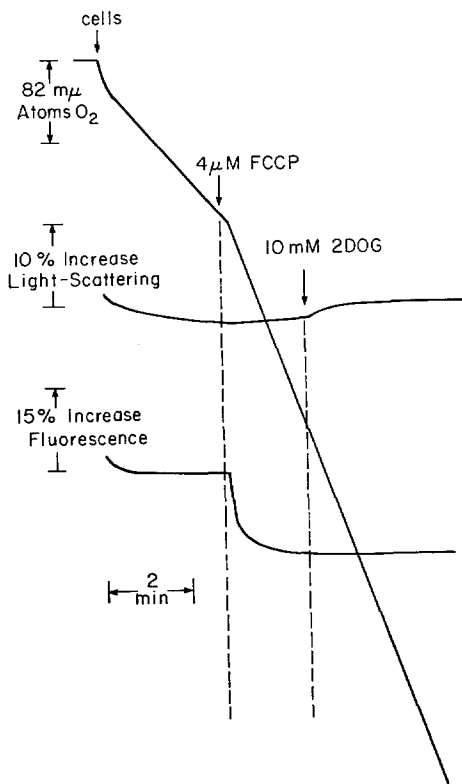


FIGURE 7 a

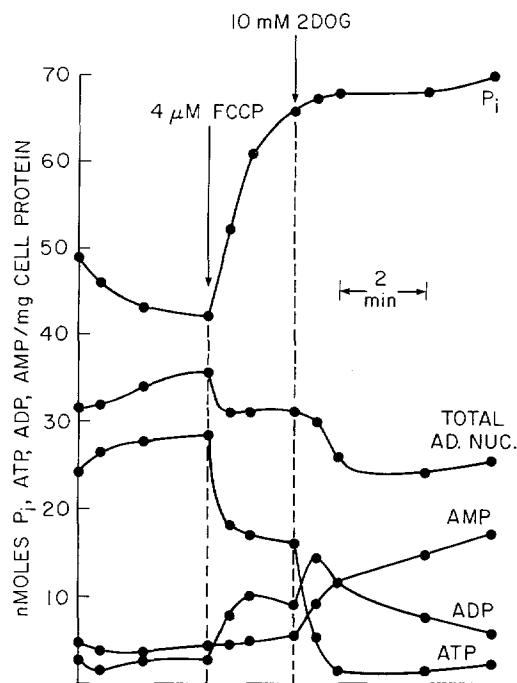


FIGURE 7 b.

FIGURE 7 Metabolic response of ascites tumor cells to addition of FCCP followed by 2DOG. Fig. 7 a, changes in oxygen consumption, fluorescence of pyridine nucleotide, and 90° light scattering. Fig. 7 b, kinetics of intracellular adenine nucleotides and P_i .

hibition of oxidative phosphorylation. This relationship is supported further by data presented in Fig. 12. When 0.8 μg of oligomycin/mg cell protein is permitted to penetrate for longer periods of time (3 min) as compared to the previous experiment (1.5 min), it completely prevents the 2DOG-induced light scattering increase (Fig. 12 a) and the orthodox \rightarrow condensed ultrastructural transformation in the mitochondria of intact cells. Oligomycin was present from zero time in this experiment. Paralleling this inhibition of structural transformation is a total inhibition of ATP synthesis, as shown in Fig. 12 b as a failure of 2DOG to decrease the intracellular level of P_i . That 2DOG gains entrance to the cells and is phosphorylated under these inhibitory conditions but fails to stimulate ATP synthesis is confirmed by the precipitous decrease in the intracellular ATP level and the unusually large and rapid increase in the intracellular ADP level after 2DOG addition (Fig. 12 b).

DISCUSSION

Generation of Intracellular ADP by 2-Deoxyglucose

The purpose of this investigation has been to analyze the ultrastructure of mitochondria as it relates to energy metabolism in the intact cell. To this end, we have monitored continuously and synchronously the respiratory rate, reduction-oxidation of mitochondrial pyridine nucleotide, light scattering, and ultrastructure of mitochondria in intact ascites tumor cells during the rapid induction of oxidative phosphorylation. We have, in addition, monitored the kinetics of intracellular ATP, ADP, AMP, and P_i , via direct enzymatic analysis, in order to confirm the occurrence of induced intracellular oxidative phosphorylation.

Although we have used both glucose and 2DOG as ADP-generating monosaccharides, the use of the nonglycolyzable 2DOG was preferred since it

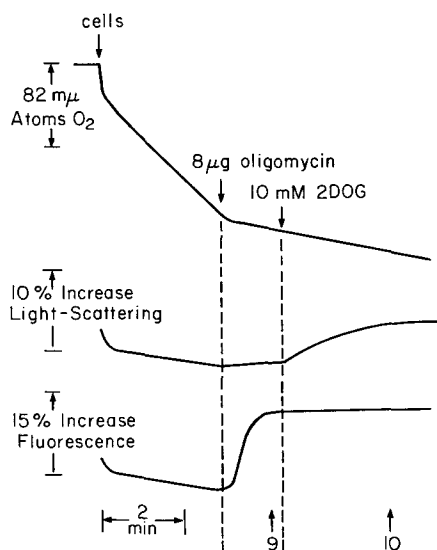


FIGURE 8 a

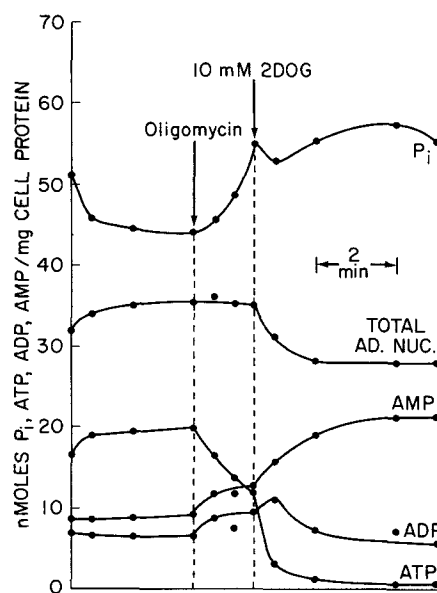


FIGURE 8 b

FIGURE 8 Metabolic response of ascites tumor cells to addition of oligomycin ($0.8 \mu\text{g}/\text{mg}$ of cell protein) followed by 2DOG. Fig. 8 a, changes in oxygen consumption, fluorescence of pyridine nucleotide, and 90° light scattering. Numbered arrows refer to microsamples of cells fixed for electron microscopy and shown in Figs. 9 and 10. Fig. 8 b, kinetics of intracellular adenine nucleotides and P_i .

generates intracellular ADP uncomplicated by the effects of glycolysis and collateral metabolic pathways which occur in the cytosol during the uptake of glucose. 2DOG-6-P, the hexokinase reaction product of DOG, is not metabolized further in the ascites tumor cell (9) and therefore the ADP generated via the hexokinase step is not rephosphorylated to ATP by glycolytic activity. This results in a noncompetitive, rapid availability to the mitochondria of the ADP generated in the hexokinase reaction. In addition, 2DOG-6-P does not inhibit hexokinase activity (22) as does G-6-P. Since 2DOG does not lead to the formation of pyruvic and lactic acids, it does not complicate the interpretation of mitochondrial respiratory state with respect to the arrival of ADP at the mitochondria and does not lead to a lowering of intracellular pH as does glucose (9).

Use of 2DOG has permitted us to monitor changes in the redox state of pyridine nucleotide of the mitochondria in intact ascites tumor cells by fluorescence emission (15) uncomplicated by glycolytic-induced changes in pyridine nucleotide in the cytosol. It has been observed that 2DOG is more effective than other hexoses, including glucose, in effecting light scattering increases in ascites tumor cells (13). In agreement with this finding, we have observed the amplitude of ultrastructural transformation in mitochondria in intact ascites tumor cells to be more pronounced with use of 2DOG than with glucose.

It should be mentioned here that continued incubation of ascites tumor cells in the presence of 2DOG has been shown to result in the degradation of intracellular adenine nucleotide stores by dephosphorylation and deamination to inosine (23). This degradation may also occur in the presence of glucose and appears to be related to low levels of intracellular P_i (24). We have, therefore, purposely limited our studies to short-term incubations. We would point out that in our experiments, where the addition of 2DOG induces a rapid orthodox \rightarrow condensed transformation in mitochondria, the intracellular adenine nucleotide, i.e. the sum of the endogenous levels of ATP, ADP, and AMP remains constant at $30 \text{ nmoles}/\text{mg}$ of cell protein (Fig. 2 b) or falls only $3 \text{ nmoles}/\text{mg}$ of protein (Fig. 8 b). In addition, it is clear that greater degradation of intracellular adenine nucleotide, e.g. $10 \text{ nmoles}/\text{mg}$ of protein over a period of 6.5 min (Fig. 12 b), results neither in a change of mitochondrial ultrastructure nor in an

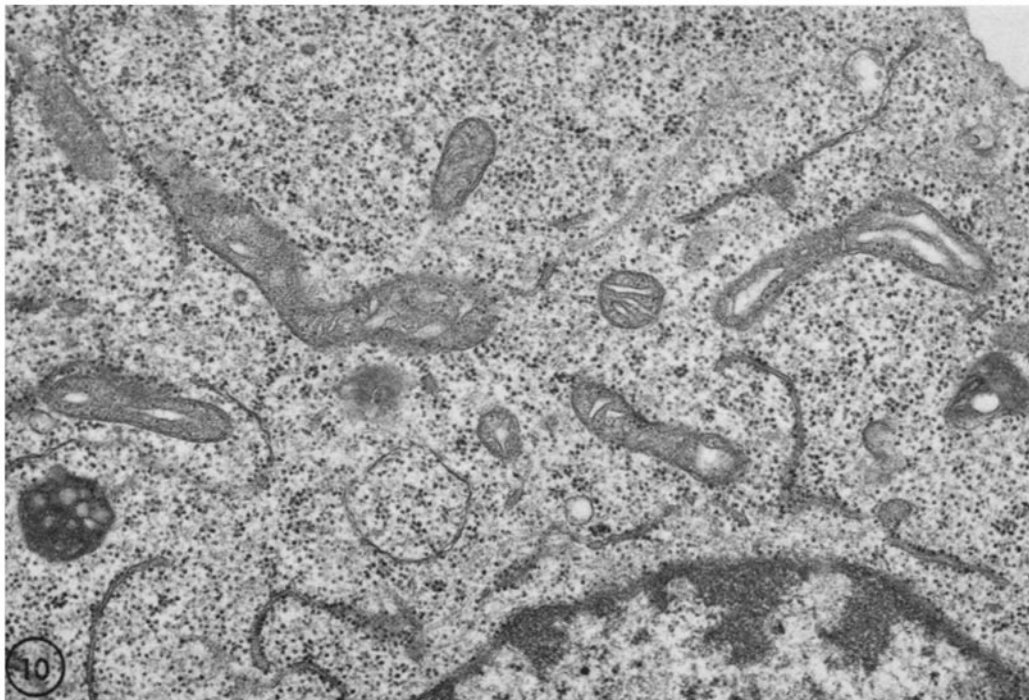
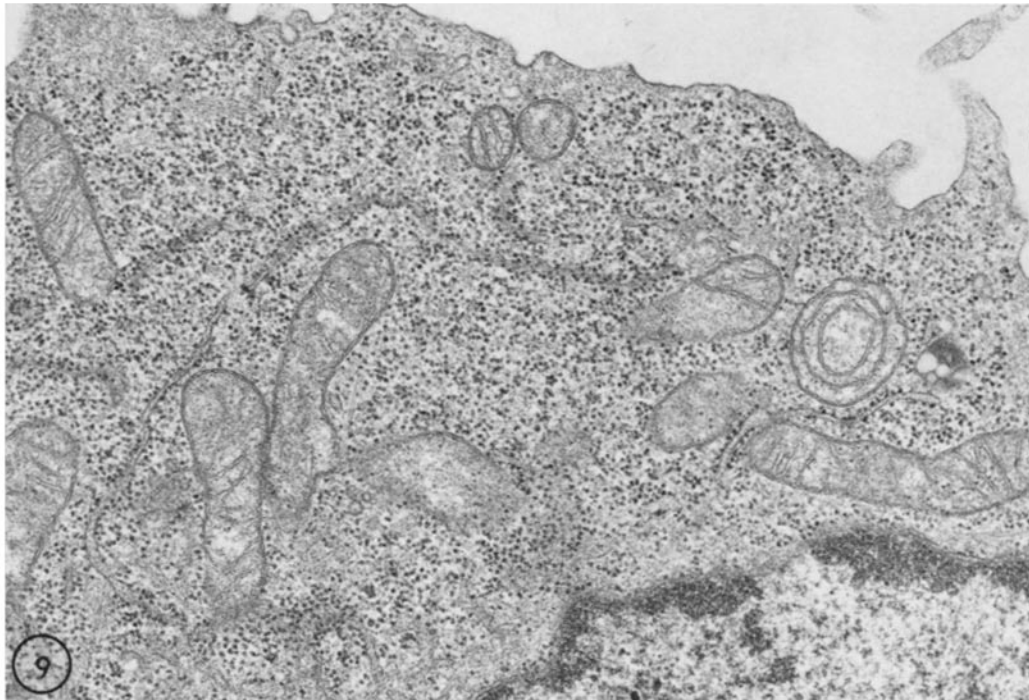


FIGURE 9 Intact ascites tumor cell fixed 1.5 min after addition of oligomycin. Mitochondria remain orthodox (See arrow 9 in Fig. 8 a). $\times 26,000$.

FIGURE 10 Intact ascites tumor cell fixed 3 min after addition of 2DOG. Oligomycin was allowed to react with cells 1.5 min before addition of 2DOG. Mitochondria show definite, but less than maximal condensation (See arrow 10 in Fig. 8 a). $\times 26,800$.

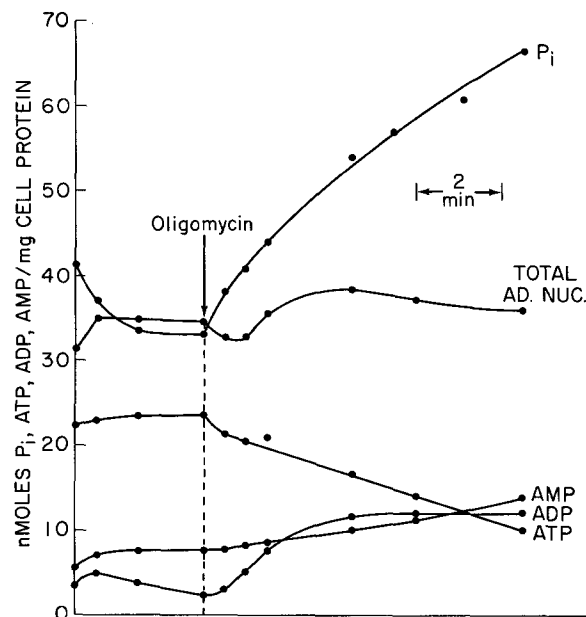


FIGURE 11 Kinetics of intracellular adenine nucleotides and P_i in intact ascites tumor cells in response to addition of oligomycin ($0.8 \mu\text{g}/\text{mg}$ of cell protein). 2DOG was not added after oligomycin as it was in the experiment of Fig. 8 *b*.

increase in 90° light scattering (Fig. 12 *a*). Thus, we have found no positive relationship between ultrastructural transformation in mitochondria and degradation of intracellular adenine nucleotide.

Ultrastructural Transformation Related to Light Scattering

In earlier studies of isolated liver mitochondria, we showed the state 4-induced orthodox conformation to transform to the condensed conformation in less than 20 sec after the addition of ADP (2). In the present study, a less than maximum orthodox \rightarrow condensed ultrastructural transformation (Fig. 4) was found to occur in the mitochondria in all cells in less than 6 sec after the intracellular generation of ADP by 2DOG. *Maximal* condensation (Fig. 5) of the mitochondria, however, occurs in only 25% of the cells within the first 6 sec (Fig. 6). Thus, whereas the orthodox \rightarrow condensed $t_{1/2}$ was less than 6 sec, the orthodox \rightarrow *maximally* condensed $t_{1/2}$ was 25 sec (Fig. 6). Not only did the rise in the 90° light scattering signal parallel the kinetics of the orthodox \rightarrow *maximally* condensed transformation, but the light scattering rise also showed a $t_{1/2}$ of 25 sec in intact ascites tumor cells (Fig. 2 *a*). Since our data reveal that the mitochondria of any one cell condense syn-

chronously, it becomes apparent that the kinetics of the light scattering increase reports a temporal summation of the various rates of the orthodox \rightarrow *maximally* condensed transformation in the mitochondria of the entire cell population.

In conclusion, we point out that only electron microscopy has revealed that all the mitochondria in the ascites tumor cells condense within 6 sec after addition of 2DOG. The 90° light scattering signal gave no indication of this rapid condensation of relatively low amplitude (Fig. 4) since the light scattering was found to rise in temporal agreement with the summation of the number of mitochondria in the *maximally* condensed state (Fig. 5).

Ultrastructural Transformation Related to Oxidative Phosphorylation

We have consistently observed that the addition of 2DOG to intact uninhibited ascites tumor cells initiates a rapid orthodox \rightarrow condensed ultrastructural transformation in all mitochondria. That 2DOG also initiates a rapid burst of oxidative synthesis of ATP in these cells is established by: (*a*) a twofold increase in oxygen consumption; (*b*) a rapid decrease in the reduction of mitochondrial pyridine nucleotide; (*c*) a decrease in total intracellular ATP; (*d*) an increase in total intracellular

ADP; and (e) a pronounced decrease in intracellular P_i .

Although all of these changes are characteristic of hexose-induced oxidative phosphorylation in

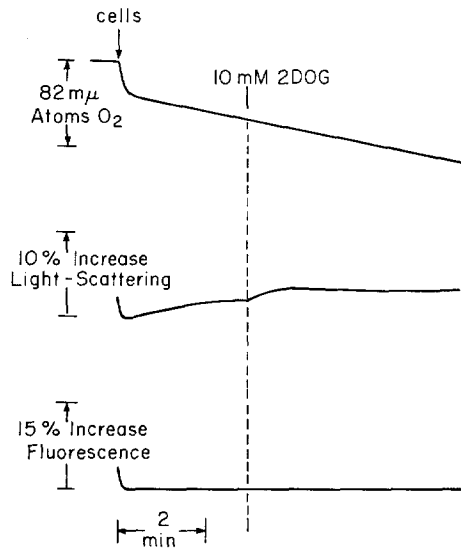


FIGURE 12 a

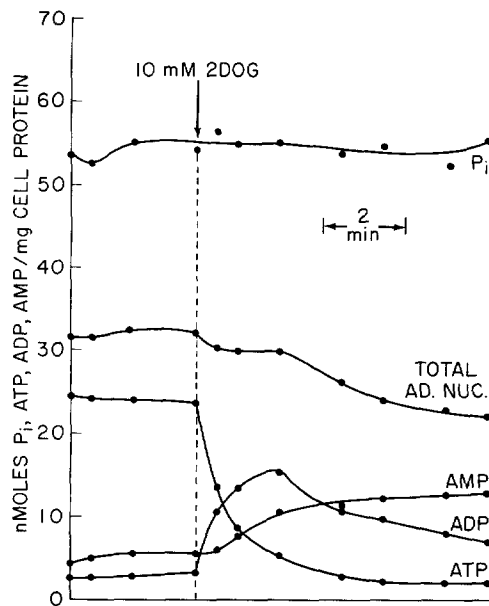


FIGURE 12 b

FIGURE 12 Metabolic response of ascites tumor cells to oligomycin followed by 2DOG. Oligomycin ($0.8 \mu\text{g}/\text{mg}$ cell protein), present at zero time, was allowed to react with cells 3 min before addition of 2DOG. Fig. 12 a, changes in oxygen consumption, fluorescence of pyridine nucleotide, and 90° light scattering. Fig. 12 b, kinetics of intracellular adenine nucleotides and P_i .

intact cells, the most revealing change is the decrease in intracellular P_i . It is important to note that 2DOG sequesters intracellular P_i indirectly by removal of the terminal high-energy phosphate of ATP. Since 2DOG generates intracellular ADP in this way, we have been able to follow ADP-initiated oxidative phosphorylation directly by monitoring the removal of intracellular P_i by the mitochondria (Fig. 2 b). It should be pointed out that although 2DOG induces ATP synthesis by mitochondria in intact cells, it converts cytosolic ATP to ADP at a rate which is faster than the generated ADP can be rephosphorylated by the mitochondria. The total cellular level of ATP, therefore, falls after the addition of the hexose (Fig. 2 b).

Our present data support and extend our previous findings, that oxidative phosphorylation in isolated liver mitochondria parallels an orthodox \rightarrow condensed ultrastructural transformation (1, 2). It is clear from our present observations that the orthodox \rightarrow condensed transformation occurs in mitochondria with the initiation of oxidative phosphorylation in the intact ascites tumor cell. This transformation is totally inhibited by uncoupling levels of FCCP, Dicumarol, and DNP as we found previously in isolated liver mitochondria. We have observed $4 \mu\text{M}$ FCCP to be required for maximal uncoupling in ascites tumor cells (Fig. 7 b). In preliminary studies, our data showed that $1-2 \mu\text{M}$ FCCP maximally stimulates respiration in ascites tumor cells (25); however, subsequent use of analysis of intracellular adenine nucleotides has revealed that $2 \mu\text{M}$ FCCP does not completely uncouple these cells. Analysis of adenine nucleotides has also permitted us to verify the entrance of 2DOG into uncoupled cells by observing the disappearance of intracellular ATP and generation of ADP and AMP at this time (Fig. 7 b).

The use of partial and complete inhibition of oxidative phosphorylation by oligomycin in ascites tumor cells illustrates well the positive relationship between mitochondrial ultrastructure and ATP synthesis in these cells. In a number of experiments, we have found adenine nucleotide and P_i analysis to reveal that some ATP synthesis occurs in cells treated with oligomycin for 2 or less min (Fig. 8 b). We have observed that a less than maximal orthodox \rightarrow condensed ultrastructural transformation and a partial rise in 90° light scattering occurs after the addition of 2DOG in the presence of oligomycin only when some ATP synthesis takes place (Figs. 8-10). Longer incubations in the

presence of oligomycin, i.e. 3 min or more, were found to abolish completely 2DOG-induced oxidative phosphorylation (Fig. 12 *b*) as well as the 2DOG-induced orthodox \rightarrow condensed transformation and light scattering increase (Fig. 12 *a*). After 2 min of oligomycin incubation, 2DOG-induced ATP synthesis occurs because of an incomplete inhibition by the oligomycin, the basis of which is most likely due to a limited penetration time under the conditions of the experiments. This suggestion is supported by our finding that raising the oligomycin concentration from 0.8 to 1.7 $\mu\text{g}/\text{mg}$ of cell protein does not influence the relationship between incubation time and complete inhibition of ATP synthesis.

We conclude from the data presented in this communication that an orthodox \rightarrow condensed ultrastructural transformation in the mitochondria in intact ascites tumor cells is linked to induced oxidative phosphorylation in these cells.

The authors thank Doctors Mark Woods and Dean Burk for providing us with Ehrlich ascites tumor cells to establish our cultures. We thank Miss Margit Lucskay and Mr. C. Elwood Claggett for their expert technical assistance.

This study was supported by National Science Foundation Grant GB-18085, and American Cancer Society Grant IN-11J.

Received for publication 21 January 1971, and in revised form 3 May 1971.

REFERENCES

1. HACKENBROCK, C. R. 1966. *J. Cell Biol.* **30**:269.
2. HACKENBROCK, C. R. 1968. *J. Cell Biol.* **37**:345.
3. HACKENBROCK, C. R., and A. I. CAPLAN. 1969. *J. Cell Biol.* **42**:221.
4. GREEN, D. E., J. ASAI, R. A. HARRIS, and J. PENNISTON. 1968. *Arch. Biochem. Biophys.* **125**:684.
5. GOYER, R. A., and M. KRALL. 1969. *J. Cell Biol.* **41**:393.
6. JASPER, D. K., and J. R. BRONK. 1968. *J. Cell Biol.* **38**:277.
7. BUFFA, P., V. GUARRIERA-BOBYLEVA, U. MUSCATELLO, and I. PASQUALI-RONCHETTI. 1970. *Nature (London)*. **226**:272.
8. WILLIAMS, C. H., W. J. VAIL, R. A. HARRIS, M. CALDWELL, and D. E. GREEN. 1970. *J. Bioenerg.* **1**:147.
9. IBSEN, K. H., E. L. COE, and R. W. MCKEE. 1958. *Biochim. Biophys. Acta.* **30**:384.
10. CHANCE, B., and B. HESS. 1959. *J. Biol. Chem.* **234**:2421.
11. YUSHOK, W. D. 1964. *Cancer Res.* **24**:187.
12. MAITRA, P. K., and B. CHANCE. 1965. In *Control of Energy Metabolism*. B. Chance, R. W. Estabrook, and J. R. Williamson, editors. Academic Press Inc., New York. 157.
13. PACKER, L., and R. H. GOLDBERGER. 1960. *J. Biol. Chem.* **235**:1234.
14. SZARKOWSKA, I. L., and M. KLINGENBERG. 1963. *Biochem. Z.* **338**:674.
15. ESTABROOK, R. W. 1962. *Anal. Biochem.* **4**:231.
16. CHANCE, B., and G. R. WILLIAMS. 1956. *Advan. Enzymol.* **17**:65.
17. CLARK, L. C., JR., R. WOLF, D. GRANGER, and Z. TAYLOR. 1953. *J. Appl. Physiol.* **6**:189.
18. WENNER, C. E., E. J. HARRIS, and B. C. PRESSMAN. 1967. *J. Biol. Chem.* **242**:3454.
19. PRESSMAN, B. C. 1967. *Methods Enzymol.* **10**:714.
20. ADAM, H. 1963. In *Methods of Enzymatic Analysis*. H. Bergmeyer, editor. Academic Press Inc., New York. 539, 573.
21. DRYER, R. L., A. R. TAMMES, and J. I. ROUTH. 1957. *J. Biol. Chem.* **225**:177.
22. ROSE, I. A., and J. V. B. WARMS. 1967. *J. Biol. Chem.* **242**:1635.
23. MCCOMB, R. B., and W. D. YUSHOK. 1964. *Cancer Res.* **24**:198.
24. WU, R., and E. RACKER. 1963. In *Control Mechanisms in Respiration and Fermentation*. B. Wright, editor. Ronald Russ Company, New York. 265.
25. HACKENBROCK, C. R., and T. G. REHN. 1970. In *Microscopie Electronique*. P. Favard, editor. Society Francaise de Microscopie Electronique, Paris. **3**:143.